Enhanced Performance of Cross-Flow Savonius Turbines at Low Current Velocity: A Numerical Investigation on the Influence of Deflector Configurations

Poboljšane performanse Savoniusovih turbina s križnim protokom pri niskoj brzini struje: Numeričko istraživanje utjecaja konfiguracija deflektora

Dendy Satrio*
Institut Teknologi Sepuluh Nopember
Surabaya, Indonesia
E-mail: dendy.satrio@its.ac.id

Rizandhi Aulia Adipradana
Institut Teknologi Sepuluh Nopember
Surabaya, Indonesia
E-mail: rizandhi23@gmail.com

Muhammad Asroril Mubarok
Institut Teknologi Sepuluh Nopember
Surabaya, Indonesia
E-mail: 6020251008@student.its.ac.id

Maktum Muharja
Institut Teknologi Sepuluh Nopember
Surabaya, Indonesia
E-mail: maktum@its.ac.id

Tuswan
Universitas Diponegoro
Semarang, Indonesia
E-mail: tuswan@lecturer.undip.ac.id

Muhammad Luqman Hakim
Universitas Diponegoro
Semarang, Indonesia
E-mail: mluqmanhak@lecturer.undip.ac.id

Nik Ahmad Ridhwan
Universiti Teknologi Malaysia
Johor, Malaysia
E-mail: ridhwan@utm.my

Madi
Institut Teknologi Sumatera
South Lampung, Indonesia
E-mail: madi@tse.itera.ac.id

Abdi Ismail
National Research and Innovation Agency (BRIN)
Banten, Indonesia
E-mail: abdiismail1993@gmail.com

Siti Musabikha
National Research and Innovation Agency (BRIN)
Banten, Indonesia
E-mail: siti089@brin.go.id

https://doi.org/10.17818/NM/2026/1.2
UDK 621.125(26.07)
Original scientific paper / *Izvorni znanstveni rad*
Paper received / *Rukopis primljen:* 24. 11. 2025.
Paper accepted / *Rukopis prihvaćen:* 24. 2. 2026.

Abstract

In Indonesia, ocean currents represent a promising resource and one technology that can be used to harness them is the Savonius turbine. Although the vertical-axis Savonius turbine has been widely explored due to its ability to operate at low flow velocities, research on the cross-flow type remains limited. This study analyzed the influence of adding a deflector and placement variations on the performance of a cross-flow Savonius turbine. The turbine was tested with several deflector configurations, including different distances 0.22, 0.23, 0.24, and 0.33 m from the turbine, to evaluate their influence on performance. The deflector was designed to redirect flow to avoid the returning blade while strengthening the advancing blade, thereby enhancing energy capture. A numerical investigation was conducted using Computational Fluid Dynamics (CFD). The results of adding the deflector significantly improved the turbine performance in terms of its torque (Ct) and power coefficients (Cp) by 44%. The optimal configuration was obtained at a deflector distance of 0.23 m with a Tip Speed Ratio (TSR) of 0.739, yielding a coefficient of power of 0.289. This study indicates that proper deflector positioning can effectively improve the performance of a cross-flow type Savonius turbine.

KEY WORDS

Ocean renewable energy
Savonius turbine
Cross-flow turbine
Deflector
CFD

Sažetak

U Indoneziji oceanske struje predstavljaju obećavajući resurs, a jedna od tehnologija koja se može koristiti za njihovo iskorištavanje jest Savoniusova turbina. Iako je Savoniusova turbina s vertikalnom osi naširoko istražena zbog svoje sposobnosti rada pri malim brzinama strujanja, istraživanja o tipu križnog strujanja i dalje su ograničena. Ovaj rad analizira utjecaj dodavanja deflektora i varijacija postavljanja na performanse Savoniusove turbine s križnim protokom. Turbina je testirana s nekoliko konfiguracija deflektora, uključujući različite udaljenosti od turbine (0,22 m, 0,23 m, 0,24 m i 0,33 m) kako bi se procijenio njihov utjecaj na performanse. Deflektor je dizajniran za preusmjeravanje protoka kako bi se izbjegla povratna lopatica, dok se istovremeno ojačava djelovanje na naprednu lopaticu, čime se poboljšava hvatanje energije. Numeričko istraživanje provedeno je korištenjem računalnom dinamikom fluida (CFD). Rezultati su pokazali da je dodavanje deflektora značajno poboljšalo performanse turbine u smislu okretnog momenta (Ct) i koeficijenta snage (Cp) za 44%. Optimalna konfiguracija postignuta je pri udaljenosti deflektora od 0,23 m s omjerom brzine vrtnje (TSR) od 0,739, što je rezultiralo koeficijentom snage od 0,289. Ovaj rad ukazuje da pravilno pozicioniranje deflektora može učinkovito poboljšati performanse Savoniusove turbine s križnim protokom.

KLJUČNE RIJEČI

obnovljivi izvori energije oceana
Savoniusova turbina
turbina s križnim protokom
deflektor
CFD (računalna dinamika fluida)

1. INTRODUCTION / *Uvod*

The energy crisis has become a global concern, particularly in relation to the increasing demand for electrical energy [1], [2]. In daily life, electricity is indispensable, as technological advancements continue to increase energy dependence [3]. However, fossil fuel reserves, especially petroleum, are depleting and predicted to run out in the coming years. As a result, renewable energy has emerged as a sustainable alternative, offering resources that are naturally

* Corresponding author

replenished [4]. This is supported by the addition of installed renewable energy capacity to 876.5 MW in the first semester of 2025, a 15% increase by the Ministry of Energy and Mineral Resources (ESDM) [5]. Located between two oceans and along the equator, Indonesia possesses abundant renewable energy potential [6].

Among various renewable energy resources, ocean current energy is favorable for Indonesia [7]. Ocean current energy is one of the most promising renewable energy sources. There are 17 potential locations for ocean current energy in Indonesia [5], including several narrow straits. The highest-potential currents in the Larantuka Strait have speeds ranging from 1.1 to 3.4 m/s [6]. Several other locations in low current velocity, namely the Sunda Waters, Lombok, Alas, Sugi Strait, and Palawan Waters, have average currents exceeding 0.5 m/s and maximum currents exceeding 1 m/s [8]. Furthermore, ocean current energy is environmentally friendly and predictable, making it a practical choice for electricity generation.

Ocean current turbines transduce the water's kinetic energy into electrical power, offering advantages such as low noise, minimal land use, and reliable energy capture. However, challenges remain in durability, maintenance, and cost, among the several types: horizontal-axis [7], [9], vertical-axis [10], [11], [12], and cross-flow [13]. The cross-flow turbine is particularly attractive for low-speed currents, making it suitable for waters such as those in Indonesia [8]. In line with this potential, the Savonius turbine, characterized by its simple design, self-starting capability, and adaptability to floating systems, represents a promising configuration for cross-flow applications [14].

Building on these strengths, cross-flow Savonius turbines combine the advantages of operating efficiently in low-speed currents with ease of construction and deployment, making them especially promising for Indonesian waters [15]. However, their potential has not yet been fully explored, as studies on this type of turbine remain limited compared to other turbine types. The need for further research focused on blade design, deflector placement, and array configurations to enhance their performance and support wider practical implementation [16].

Several studies have investigated methods to improve Savonius turbine performance through various modifications, including increasing the number of stages [17], varying the number of blades [18], altering the end plate geometry, and adding deflectors [19], [20]. The addition of deflectors has been shown to significantly enhance turbine efficiency; for example, [19] reported a 29.84% increase in power coefficient (Cp) at a 60° stagger angle and a 41.18% improvement when deflectors were positioned in front of the blades. At the same time, [21] demonstrated that flat-shaped deflectors yielded the highest increase of 24% compared to triangular and semicircular shapes. Similarly, [22] found that deflector placement combined with blade variation produced performance improvements of 128.36% for two-bladed and 604.62% for three-bladed configurations.

Research on deflectors has shown that the deflector angle increases turbine performance by an average of 12% [1]. Immersion depth and rotation direction also improve turbine performance [13]. Building upon these findings, this study investigated the influence of deflector and horizontal distance variation implementation on the performance improvement of a cross-flow Savonius turbine. The deflector was designed to minimize negative torque at the returning blade by redirecting the flow, while simultaneously maximizing positive torque at the advancing blade to enhance energy capture.

2. MATERIALS AND METHODS / *Materijali i metode*

2.1 Geometrical and Variations Configuration / *Geometrijske karakteristike i varijacije konfiguracije*

A deflector is an object that serves to disrupt or even deflect the flow of fluid so that it does not directly hit the turbine [15], [23]. The deflector serves as both a tool to control flow speed and a turbine protection against foreign objects. In conditions without a deflector, the turbine flow is not obstructed, so it goes directly to the returning blade, which can result in a decrease in the positive torque generated [23]. The deflector design was adapted from the configuration proposed by [17]. The turbine geometry from Golecha's study was then adopted and modified to suit the requirements of the Computational Fluid Dynamics (CFD) simulation [17]. The detailed geometry is shown in Figure 1. Figure 1 (a) for the Savonius turbine and Figure 1 (b) for the deflector, along with the specifications presented in Table 1.

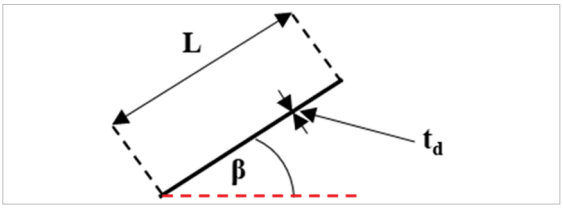

(a)

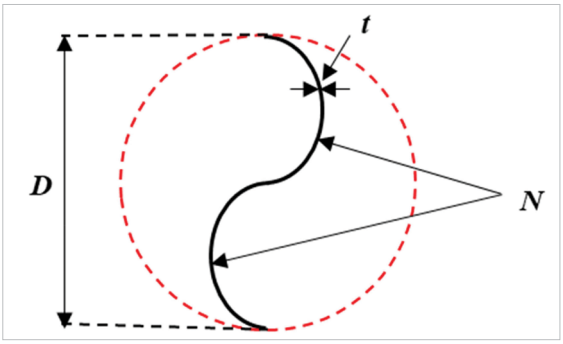

(b)

Figure 1 The geometry illustration (a) a Deflector (b) a cross-flow Savonius turbine

Slika 1. Geometrijski prikaz: (a) deflektor, (b) Savoniusova turbina s križnim protokom

In this study, the turbine was further tested under various deflector configurations with different distances from the deflector to evaluate their impact on performance. The deflector is specifically designed to strengthen the advancing blade by diverting flow away from the returning blade, thereby improving energy capture. The positioning deflector with the Savonius turbine is shown in Figure 2.

Table 1 The Savonius turbine and deflector specifications

Tablica 1. Specifikacije Savoniusove turbine i deflektora

Geometry	Variables	Symbol	Specifications
Savonius Turbine	Turbine diameter	D	0.245 [m]
	Turbine height	H	0.170 [m]
	Blade thickness	t	0.002 [m]
	Number of blades	N	2 [-]
Deflector	Deflector length	L	0.132 [m]
	Deflector height	h	0.170 [m]
	Deflector thickness	t_d	0.001 [m]
	Deflector angle	β	44 [°]
	Deflector distance	X_2	0.22, 0.23, 0.24, 0.33 [m]

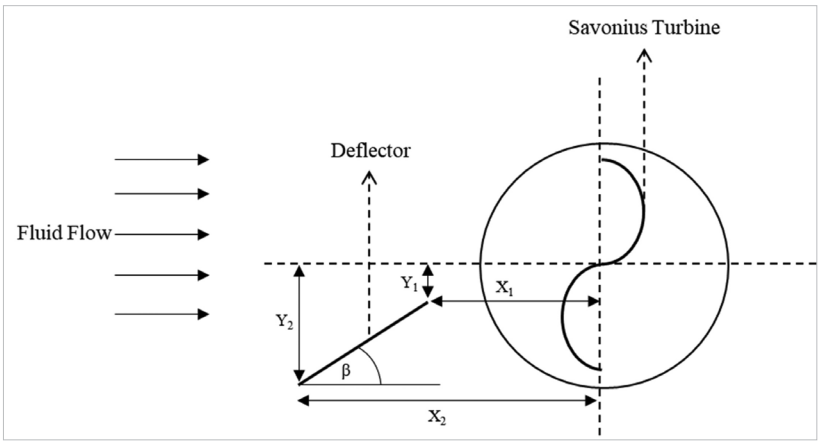

Figure 2 The Savonius turbine with deflector
Slika 2. Savoniusova turbina s deflektorom

The cross-flow Savonius turbine used in this research was designed with a turbine height (H) of 0.170 m, a blade thickness (t) of 0.002 m, and a turbine diameter (D) of 0.245 m. The rotor consisted of two blades (N = 2) arranged symmetrically to ensure balanced operation. To enhance turbine performance, a deflector was incorporated into the model with a deflector length (L) of 0.132 m, a deflector height (h) of 0.170 m, a deflector thickness (t_d) of 0.001 m, and a deflector angle (β) of 44°, while the distance from the turbine axis (X_2) was varied to evaluate its effect on flow redirection and energy capture.

This study considered variations in the deflector distance (X_2) from the turbine, set at 0.22, 0.23, 0.24, and 0.33 m as seen in Table 2. These variations were selected to examine the effect of deflector placement on flow redirection and its influence on torque and power performance [23]. The purpose of this variation is to decrease the torque acting on the returning blade while increasing the torque generated by the advancing blade. The resulting configurations provided the basis for evaluating improvements in the Ct and Cp through numerical simulations [19].

Table 2 The deflector configuration
Tablica 2. Konfiguracija deflektora

Configuration	1st	2nd	3rd	4th
X_1 [m]	0.125	0.135	0.145	0.235
X_2 [m]	0.22	0.23	0.24	0.33
y_1 [m]	0.55	0.55	0.55	0.55
y_2 [m]	0.145	0.145	0.145	0.145

2.2. Boundary Conditions and Computational Domains / *Granični uvjeti i računalne domene*

The boundary conditions at simulation are illustrated in Figure 3 and explained below, where represents the turbine diameter. The inlet is defined as a velocity inlet boundary located 10D upstream of the turbine, to ensure that the flow profile is fully developed before reaching the rotor. The outlet is defined as a pressure outlet boundary located downstream of the turbine to prevent outflow from backflowing into the rotor area. The upper and lower boundaries of the domain are treated as walls or symmetry boundaries to minimize external influences on the main flow. Meanwhile, the turbine blade surface is modelled as a no-slip wall, so the fluid velocity relative to the blade surface is zero. Additionally, deflectors are inserted into the domain at varying distances from the turbine, according to the studied configuration.

The computational domain in this study is rectangular with dimensions of 20D × 10D. The turbine is located at the centre of the domain's rotation, 5D from the inlet boundaries, and 5D from the symmetry boundaries. The turbine has a diameter of 1.2D and is surrounded by a rotary zone. The area outside this zone is designated the stationary zone. The interface between the two zones is connected via a sliding-mesh method, which accurately captures the dynamic interactions between the fluid and the rotor.

This domain setting and boundary conditions refer to the results of previous research, which have been proven effective in modelling fluid–structure interactions in Savonius turbines [23]. The inlet boundary was set with a velocity of 0.54 m/s, while the outlet was configured as the outflow direction using a symmetric

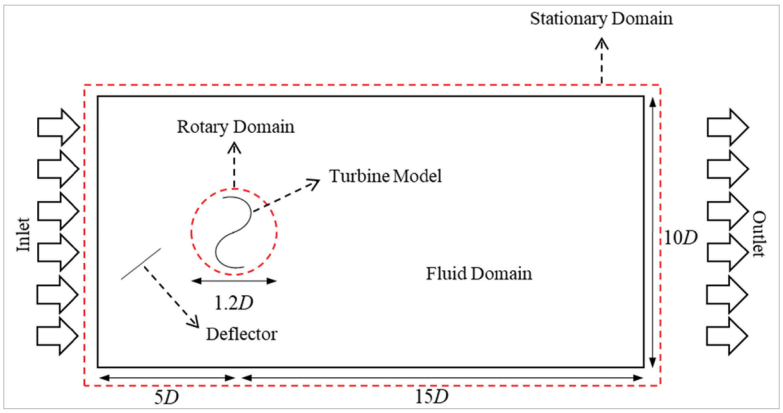

Figure 3 The boundary conditions and computational domains
Slika 3. Granični uvjeti i računalne domene

boundary condition. The downstream domain length was designed to be sufficient for capturing the wake effect generated by the turbine. This setup was determined based on the boundary condition approaches adopted in previous studies by [23].

2.3. Grid Independence and Meshing / *Neovisnost o mreži i generiranje mreže*

A grid independence study was conducted to ensure that the mesh elements used were sufficient to produce accurate simulation results. This analysis was conducted on a turbine with no flow disturbances. The simulation process started from 73,000 mesh elements and gradually increased the number to 783,000, as shown in Figure 4. Based on the analysis, 640,511 mesh elements were selected as the optimal configuration because the difference in simulation results between 640,511 and 783,000 were insignificant, while the computation time was substantially reduced. Therefore, this configuration was deemed efficient and representative for use in subsequent simulation stages.

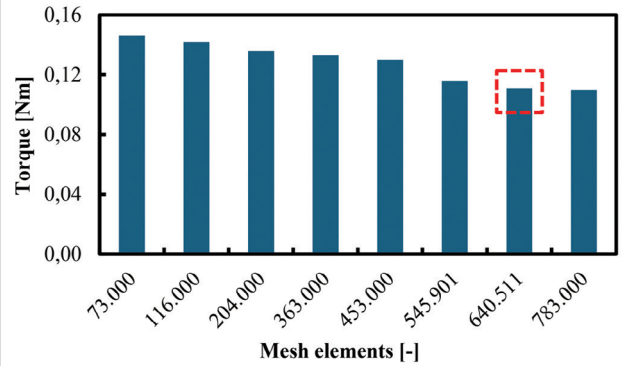

Figure 4 The grid independence study
Slika 4. Analiza neovisnosti mreže

Mesh quality is essential to gain accurate simulation results. An unstructured mesh covering the whole fluid domain was created for this investigation. From the turbine in the domain's center, the mesh elements were positioned radially in the direction of the fluid domain border. To enhance numerical accuracy in the vicinity of the turbine blades, local mesh refinement was applied, as illustrated in Figure 5. The blade surfaces were discretized using inflation layers based on the First Layer Thickness approach, with a first cell height of 3.4×10^{-5} m, up to 20 layers, a geometric growth distribution, and a growth rate of 1.05, enabling adequate resolution of the near-wall region and boundary-layer flow phenomena [24].

The 2D simulations employed the Shear Stress Transport (SST) k–ω turbulence model, selected for its proven capability to accurately capture flow separation, vortex shedding, and transitional flow phenomena that are dominant in Savonius turbine hydrodynamics. Under the present operating conditions, the flow corresponds to a Reynolds number of 1.4×10^5. The model also provides stable and reliable predictions for rotating and unsteady flows, and has been widely applied and validated in previous CFD studies of Savonius and vertical-axis turbines with similar flow characteristics. The model was implemented in its Reynolds Number formulation, allowing the viscous sublayer to be resolved explicitly without the use of wall functions. Accordingly, the mesh was designed to satisfy a target nondimensional wall distance of $y^+ < 1$ over the entire blade surface.

Post-processing results indicate that the actual y^+ values obtained were approximately 0.98 along the blade surfaces, confirming that the first computational cell lies within the viscous sublayer and ensuring reliable prediction of wall shear stress and hydrodynamic forces.

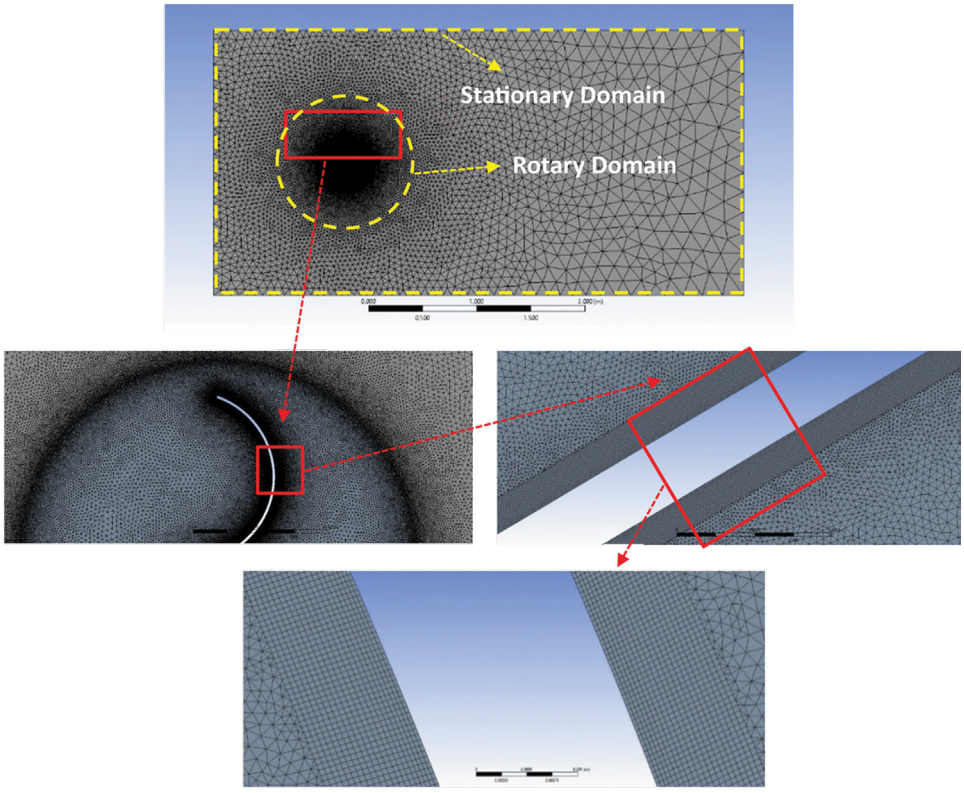

Figure 5 The mesh illustration in CFD numerical simulation
Slika 5. Ilustracija mreže u numeričkoj simulaciji CFD-a

All simulations were performed using a pressure-based, segregated solver with an absolute velocity formulation under transient flow conditions. Pressure–velocity analysis using the SIMPLE algorithm. Second-order discretization schemes were applied for pressure, momentum, and turbulence variables (k and ω), while second-order implicit time discretization was used for temporal advancement. All computations were carried out in double precision, and solution convergence was monitored using a residual threshold of 10^{-4} for the continuity, momentum, and turbulence equations [25].

2.4. Rotational Study Configurations / *Konfiguracije rotacijskih ispitivanja*

The number of turbine rotations directly influences the Number of Time Steps (NTS) used in numerical simulations. The greater the number of rotations, the higher the computational load and calculation duration. According to [26], a minimum of four rotations is required to ensure wake formation, while six rotations are recommended to achieve simulation results with a low error rate, balanced computation time, and guaranteed wake formation.

The results in Table 3 indicate that the error value relative to the previous rotation remains relatively high up to the fifth rotation. Stability is only achieved in the sixth rotation, indicated by a smaller error value and no significant differences, so the results can be considered convergent.

Table 3 The percentage error on each rotation calculation
Tablica 3. Postotno odstupanje pri svakom izračunu rotacije

Rotations [-]	Cm [-]	Torque [Nm]	Ct [-]	Cp [-]	Error [%]
1st	0.145	0.107	0.268	0.186	
2nd	0.156	0.116	0.288	0.201	-7.10%
3rd	0.182	0.135	0.338	0.235	-14.66%
4th	0.129	0.096	0.239	0.166	41.35%
5th	0.161	0.119	0.298	0.207	-19.76%
6th	0.163	0.121	0.302	0.210	-1.29%

The displays in Figure 6 show the torque distribution over rotation angles up to 2160˚. In the initial phase, torque fluctuated significantly, peaking at ±0.35 Nm due to unstable flow transient conditions. However, after passing 720˚, the torque pattern began to oscillate periodically with a relatively constant amplitude.

The behaviour shows that the system has achieved a steady-state situation in which the torque oscillation pattern no longer varies considerably between rotations. Therefore, six full rotations can be used as an optimal reference in numerical simulations of the Savonius turbine to produce representative, stable, and scientifically valid data.

In studies of Savonius and other vertical-axis turbines, it is common practice to apply time-averaging over multiple rotor revolutions to eliminate transient startup effects and ensure that the wake has fully developed, as demonstrated in previous numerical investigations [26]. Such an approach allows the phase-dependent fluctuations of torque and flow structures to converge toward a statistically representative state. In the present study, the moment coefficient was therefore evaluated based on cycle-averaged values, and the sixth full rotation was selected for averaging [13], [23] because it exhibited the smallest relative error (1.29%) and negligible variation compared to subsequent rotations. This procedure ensures that the reported torque and power coefficients correspond to a fully developed wake and a stable operating regime.

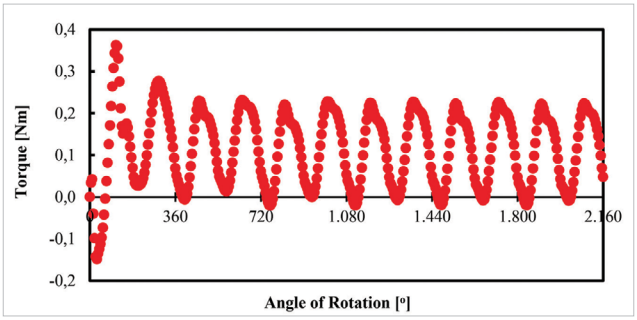

Figure 6 The torque characteristics to the angular position of the turbine
Slika 6. Karakteristike okretnog momenta u odnosu na kutni položaj turbine

2.5. Solver and Parameter Setting / *Postavke alata (solvera) i parametara*

This simulation was conducted using the sliding-mesh method under transient conditions to model the fluid flow changes during turbine rotation. The turbulence model used was the SST K-ω, as referenced in [25]. The simulation used water as the fluid, and the turbine blades were modeled as walls with standard materials built into the software. The U-RANS model was used to simulate the flow. The time step in the simulation was set to 5˚, in line with the recommended range of 1˚ to 5˚ [26]. The simulation was run for six turbine rotations, as the system had reached a stable state at this stage. The result was validated with experimental data before modifications were made using a deflector. Several key performance parameters were then established to assess turbine performance, the formulas for which are described as follows:

$$Ct = \frac{T}{0.5 \cdot \rho \cdot V^2 \cdot A \cdot R} \quad (1)$$

$$TSR = \frac{\omega \cdot R}{V} \quad (2)$$

$$Cp = Ct \cdot TSR \quad (3)$$

Equations (1) – (3) represent the dimensionless parameters used to perform the turbine. The torque value is converted into a Ct using Equation (1). Parameters used include T as the torque (Nm), ρ as the sea water density (kg/m^3), as the turbine's projection area (m^2), and R as the turbine radius (m). TSR is calculated using Equation (2), which is defined as the ratio of the turbine's angular velocity (ω, rad/s) multiplied by the turbine radius to the inlet velocity (V, m/s). Meanwhile, the Cp is obtained through Equation (3) [23].

3. RESULTS & DISCUSSION / *Rezultati i rasprava*

3.1. Validity of Simulation / *Valjanost simulacije*

Validation was performed by comparing the experimental values obtained by [17] with simulations of vertical turbines and cross-flow turbines. Validation was done by using experimental data conducted by [17]. Numerical simulations were conducted at TSR values of 0.696, 0.739, 0.800, 0.860, 0.897, 0.985, 1.015, 1.068, and 1.086. The comparison between the results from the CFD simulation and the experimental data is portrayed in Figure 7. Figure 7 (a) is a Ct chart, and Figure 7 (b) is a Cp chart.

Although the numerical results show good agreement with the experimental data reported in [17] in terms of overall trends of both Ct and Cp, some quantitative differences are observed. These discrepancies can be attributed to several factors. First, the simulations were performed using a finite time step, which may introduce temporal discretization errors, particularly in capturing instantaneous torque fluctuations. Second, the present study employed a two-dimensional (2D) cross-flow model, whereas the experimental measurements inherently included three-dimensional effects, such as tip losses and spanwise flow, which cannot be fully represented in a 2D framework. Third, the torque and power coefficients were evaluated based on cycle-averaged values over the sixth full rotor revolution, which was selected due to its minimal relative error; however, experimental data typically represent averages over longer sampling durations, potentially leading to differences in statistical convergence. Finally, experimental uncertainties, including measurement errors in torque, rotational speed, and inflow velocity control, may also contribute to the observed deviations. Despite these factors, the close correspondence in trends and magnitudes supports the validity of the numerical model for subsequent parametric studies involving deflector placement.

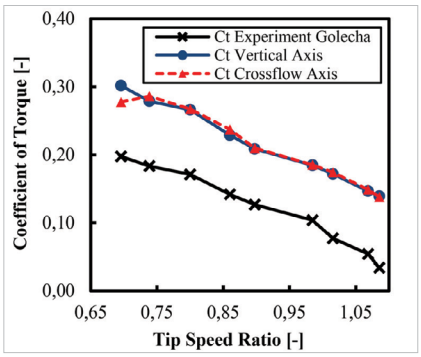

(a)

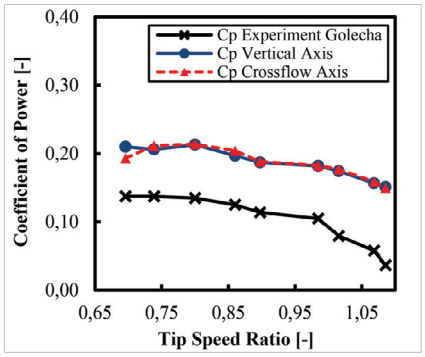

(b)

Figure 7 The comparison between numerical simulation results and experimental data for (a) Torque Coefficient (Ct) and (b) Power Coefficient (Cp) under baseline configuration without deflector

Slika 7. Usporedba rezultata numeričke simulacije i eksperimentalnih podataka za (a) koeficijent okretnog momenta (Ct) i (b) koeficijent snage (Cp) u osnovnoj konfiguraciji bez deflektora

3.2. Effects of the Turbine Deflector Addition / *Učinci dodavanja deflektora na turbinu*

A deflector placed in front of a turbine might cause the incoming flow to be disturbed, which might alter the turbine's spin. Because of this disturbance, the flow became uneven and unstable (turbulent). However, recent research has found that water vortices created by the movement or shape of the foil can actually improve turbine performance [27]. Previous experimental studies have shown that, at low flow velocities, the initiation of rotation in a Savonius turbine is strongly influenced by the relative interaction between the incoming flow and the advancing and returning blades. However, when the flow primarily impinges on the returning blade, the resulting pressure distribution produces insufficient net torque to initiate rotation. In contrast, when the flow is favourably directed toward the advancing blade, a larger pressure differential is established between the concave and convex blade surfaces, generating a positive starting torque and enabling rotor rotation even at the same flow velocity [23].

The deflector is placed to obstruct the turbine. Deflectors serve to direct fluid flow before it reaches the turbine area. Their placement significantly influences the flow characteristics that impact the turbine. The deflector can increase or decrease the flow velocity at the advancing or returning blades, depending on its installation configuration. The deflector used, according to [17] has a deflector configuration with a distance of $X_2 = 0.23$ m, $X_1 = 0.135$ m, a beta angle (β) of 44°, and $Y_2 = 0.145$ m.

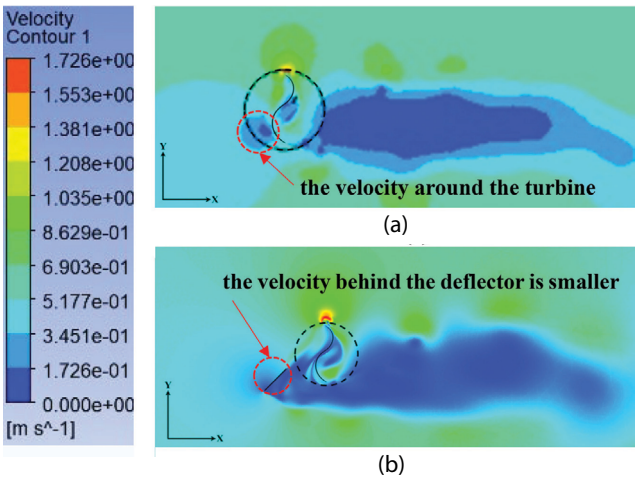

(a)

(b)

Figure 8 The velocity magnitude contour cross-flow (a) without deflector, (b) with deflector

Slika 8. Prikaz intenziteta brzine u križnom protoku (a) bez deflektora, (b) s ugrađenim deflektorom

The numerical simulation results of the cross-flow turbine type of Savonius turbine, with and without a deflector, indicate that the Ct and Cp values for the cross-flow turbine with a deflector were higher than those for the cross-flow turbine without a deflector. Only at TSR 0.984 and 1.015, the values of Ct and Cp were greater in the cross-flow turbine without a deflector than with a deflector. The most significant increase in Ct and Cp values occurred at TSR 0.696, with a 44% increase.

The velocity magnitude contour of simulations in Figure 8. The cross-flow Savonius turbine without a deflector is illustrated in Figure 8 (a) and with a deflector in Figure 8 (b). In the case without a deflector, the wake region behind the turbine was characterized by large-scale vortex shedding and flow separation, resulting in significant turbulence and energy dissipation. This condition reduced the effective velocity of the fluid interacting with the advancing blade, thereby limiting torque generation and overall turbine efficiency.

The installation of a deflector changed the inlet flow distribution by directing and concentrating the flow into the advancing blades, as well as suppressing the torque generated by the returning blades. The velocity contour demonstrated a more streamlined wake with reduced vortex intensity, indicating improved flow alignment through the turbine. This redirection of flow enhanced the local

velocity distribution around the blades, which in turn contributed to higher torque and power coefficients. These findings highlight the effectiveness of the deflector to increase the hydrodynamic performance of a cross-flow Savonius turbine.

3.3. Effects of the Turbine Deflector Placements / *Učinci položaja deflektora turbine*

Four variations of the deflector placement distance were carried out. Varied variables were 0.22, 0.23, 0.24, and 0.33 m. At a distance of 0.33 m, the variation was achieved by shifting the deflector 0.1 m to the left from its initial position. At a variation of 0.22 m and 0.24 m, the variation was done by shifting the deflector to the right or left 0.01 m from the initial position. The performance analysis based on the Ct across various TSR indicates that the addition of a deflector generally enhances turbine performance relative to the baseline, as seen in Figure 9.

The optimal improvement was observed at a TSR of 0.696, where the deflector positioned at 0.22 m achieved the highest Ct value of 0.41, representing a substantial increase relative to the baseline of 0.28. Similar improvements were noted at TSR values up to 0.800, although the gain diminished at higher TSR as flow separation and wake interactions became more dominant. Among the tested configurations, the 0.22 m deflector consistently demonstrated the most effective enhancement, while performance decreased significantly at 0.33 m due to reduced flow redirection efficiency. These results confirm that appropriate deflector placement plays a crucial role in optimizing energy capture, particularly at low TSR ranges where Savonius turbines are most effective.

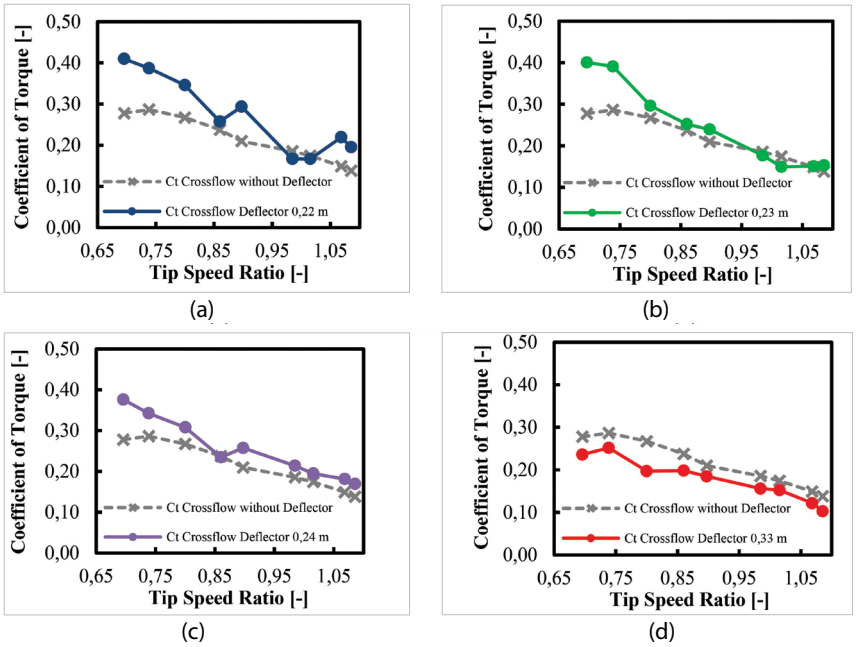

Figure 9 Ct without and with a deflector (a) 0.22 m, (b) 0.23 m, (c) 0.24 m, (d) 0.33 m

Slika 9. Koeficijent okretnog momenta (Ct) bez deflektora i s njim na udaljenosti (a) 0,22 m, (b) 0,23 m, (c) 0,24 m, (d) 0,33 m

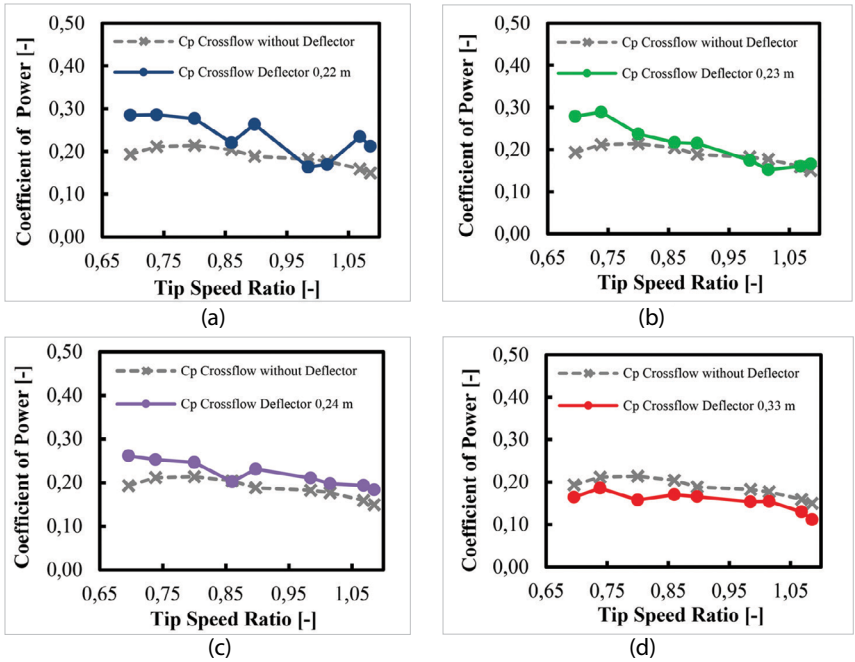

Figure 10 Cp without and with a deflector (a) 0.22 m, (b) 0.23 m, (c) 0.24 m, (d) 0.33 m

Slika 10. Koeficijent snage (Cp) bez deflektora i s njim na udaljenosti (a) 0,22 m, (b) 0,23 m, (c) 0,24 m, (d) 0,33 m

The analysis of the Cp demonstrates that integrating a deflector significantly improves turbine performance, as shown in Figure 10, particularly at lower TSR values. The most notable enhancement occured at TSR 0.739 with a Cp of 0.29 for deflector placements at both 0.22 m and 0.23 m, compared to a value of 0.21 without a deflector. Across the range of TSR values, the 0.22 m configurations consistently delivered higher Cp, confirming their effectiveness in optimizing flow redirection and energy capture. The 0.33 m placement results in the lowest performance, indicating reduced hydrodynamic efficiency due to insufficient flow guidance. At higher TSR > 0.9, performance improvements diminished across all cases, highlighting that deflector effectiveness is most pronounced in the low TSR operating range.

The addition of a deflector to a Savonius turbine aims to direct the flow more efficiently to the blades, reduce stall phenomena, and minimize energy losses due to turbulence. The deflector functions to change the angle of incidence, thereby increasing lift and optimizing the conversion of kinetic energy into mechanical energy. A comparison between Savonius turbines with and without deflectors reveals significant improvements in Cp and Ct, particularly at lower current speed variations. The use of numerical simulations enables a detailed analysis of the pressure distribution, flow, and the interaction between the deflector and the turbine blades, providing important insights for designing turbines with optimal performance.

The results of numerical simulations of cross-flow turbines with variations in the distance of deflector placement show that the distance of deflector placement affects the turbine's performance, as seen in Figure 11. Figure 11 (a) presents the Ct, while Figure 11 (b) displays the Cp. The results indicate that the variation in deflector distance has a notable effect on turbine performance. As observed in the Ct distribution, certain deflector positions are more effective in reducing torque while enhancing torque on the advancing blade. Similarly, the Cp comparison reveals that optimal deflector spacing contributes to improved energy conversion efficiency. The bar chart representation clearly emphasizes the performance differences among variations, allowing for straightforward identification of the most effective deflector distance in enhancing cross-flow turbine output.

At a deflector distance of 0.22 m, the highest performance gain occurred at TSR 0.696 and at TSR 1.069, with a performance increase of 47% from a cross-flow turbine without a deflector. At a deflector distance of 0.23 m, the largest changes in Ct and Cp occurred at TSR 0.696 with an increase in performance of 44% evaluated to a cross-flow turbine without a deflector. The highest performance gain was reached at TSR 0.696 at a deflector distance of 0.24 m, resulting in a 35% increase in performance evaluated to a turbine without a deflector. According to the research in [17], the deflector, when positioned correctly, can increase the Cp value by up to 50%.

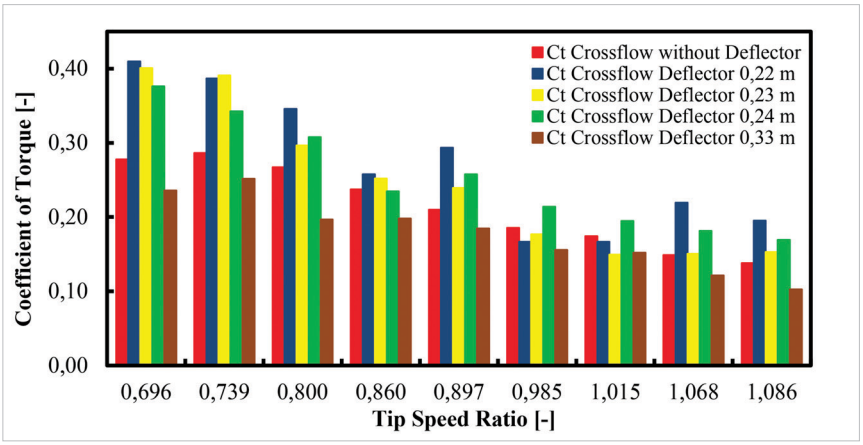

(a)

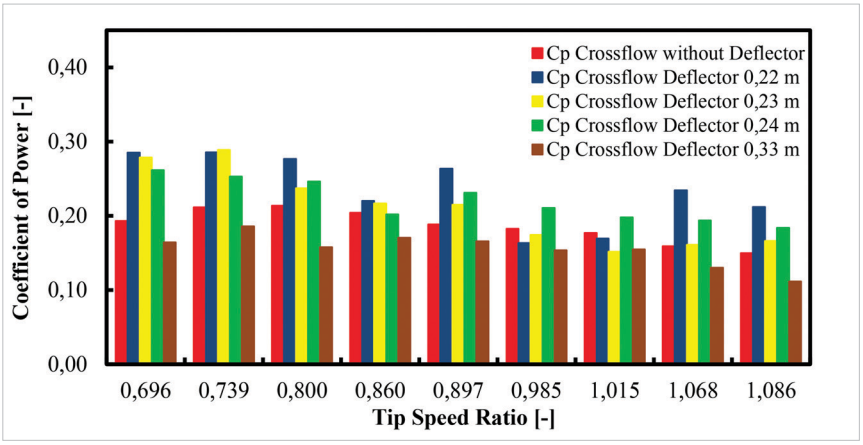

(b)

Figure 11 The Comparison of cross-flow turbine performance: (a) Ct and (b) Cp

Slika 11. Usporedba performansi turbine s križnim protokom: (a) Ct i (b) Cp

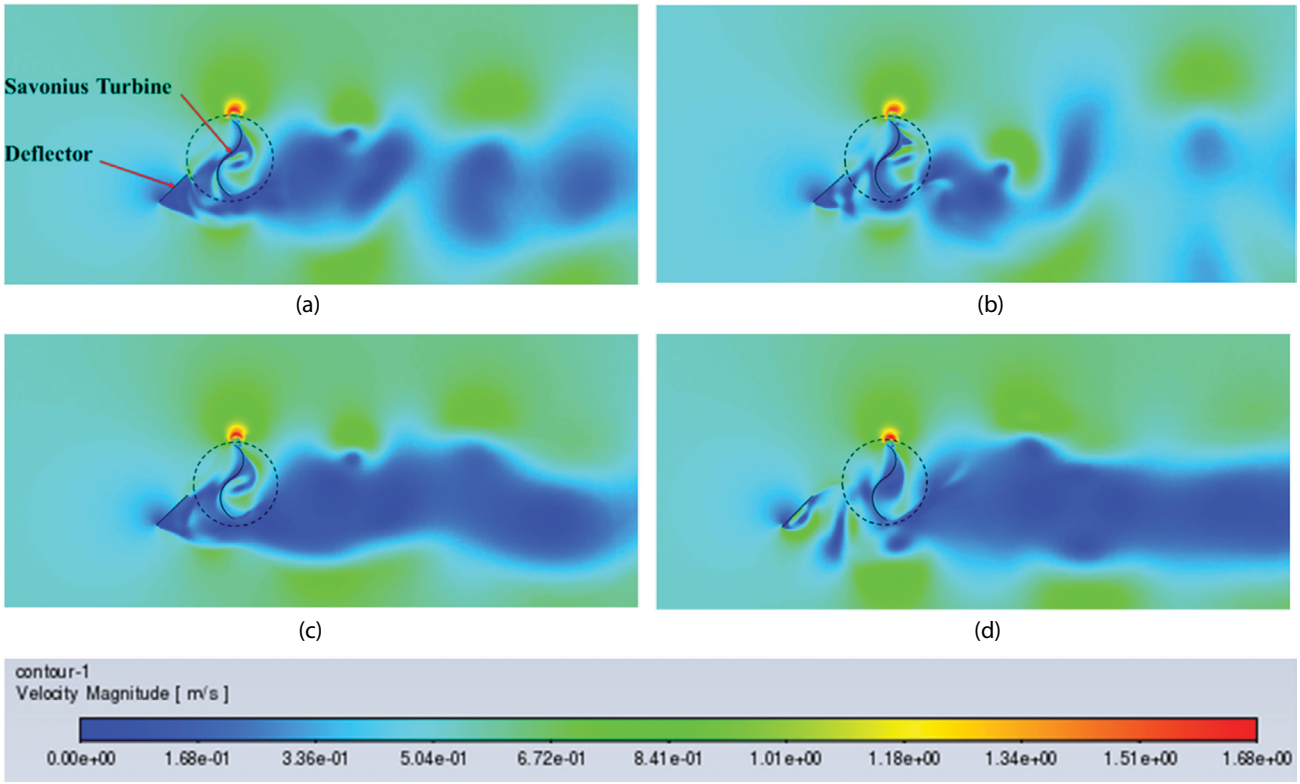

Figure 12 The velocity magnitude contour with a deflector (a) 0.22 m, (b) 0.23 m, (c) 0.24 m, (d) 0.33 m on TSR 0.800.
Slika 12. Prikaz intenziteta brzine s deflektorom na udaljenosti (a) 0,22 m, (b) 0,23 m, (c) 0,24 m, (d) 0,33 m pri TSR-u od 0,800

The average efficiency of the cross-flow turbine was reduced by 16% in all conditions when the TSR was 0.984, as evaluated to a cross-flow turbine without a deflector. At a deflector distance of 0.33 m, the turbine's performance was the lowest in comparison to that of a turbine without a deflector and a turbine with a deflector at other distances. The largest changes occurred in TSR 0.800 and TSR 1.086, with a 26% decrease compared to cross-flow turbines without deflectors.

On the contour with a TSR of 0.800, the resulting turbine rotation looks relatively stable. The flow behind the turbine indicates a reasonably good pattern, with minimal turbulence. In Figure 12, the velocity magnitude contours illustrate the impact of deflector placement on the flow characteristics around the turbine. The deflector successfully rerouted the incoming flow toward the returning blade at a spacing of 0.22 m, t, as illustrated in Figure 12 (a). This results in a concentrated wake formation and a strong velocity gradient, resulting in a 29% increase in Cp. A slight increase in distance to 0.23 m, as shown in Figure 12 (b), produced a more balanced flow distribution, reducing recirculation and enhancing momentum transfer to the turbine blades.

The deflector is positioned at 0.24 m in Figure 12 (c), the flow separation appears more stabilized, with an elongated wake region indicates smoother velocity recovery downstream.

In contrast, at a deflector spacing of 0.33 m in Figure 12 (d), the deflector's effectiveness decreases. This is evident from the wider and less directional downstream flow structure. The flow contours indicate that the flow diverted by the deflector spreads too quickly, so that the flow has not fully recovered by the time it reaches the rotor. Consequently, momentum transfer to the blades is less effective. Furthermore, the vortices formed at this spacing are diffuse and disorganized, thereby weakening the pressure difference between the blades. This condition results in a 26% decrease in the power coefficient. In contrast to the 0.22 m configuration, the more focused flow diversion results in more effective flow–blade interaction and increases energy capture. These findings confirm that deflector placement is a key parameter in improving the performance of Savonius turbines, particularly under low TSR operating conditions.

At TSR 0.800, the deflector distance affected the resulting turbulence. The turbulence intensity contours indicated that the distance of the deflector was directly proportional to the turbulence produced. At a deflector distance of 0.33 m, the turbulence produced was the largest when compared to a distance of 0.22, 0.23, and 0.24 m.

Figure 13 presents the turbulence intensity contours downstream of the deflector with four different lengths. The flow field visualization demonstrates the development of vortex shedding and the subsequent dissipation of turbulent structures along the wake region. For the 0.22 m deflector in Figure 13 (a), the turbulence intensity was primarily concentrated near the trailing edge, forming compact and periodic vertical structures that indicate more stable vortex shedding with well-defined shear layer interaction. The flow was characterized by larger vortices with a higher intensity, which were distributed further downstream as a result of the improved interaction between the main flow and the separated shear layer, in contrast to the 0.23 m depicted in Figure 13 (b).

At 0.24 m in Figure 13 (c), the contours revealed larger but less coherent vortices with rapid dissipation of turbulent energy, suggesting reduced stability of vortex shedding. In contrast, at 0.33 m in Figure 13 (d), the turbulence intensity became more diffused with large-scale structures of lower intensity, indicating more substantial dissipation of turbulent kinetic energy and reduced wake coherence. Overall, the deflector

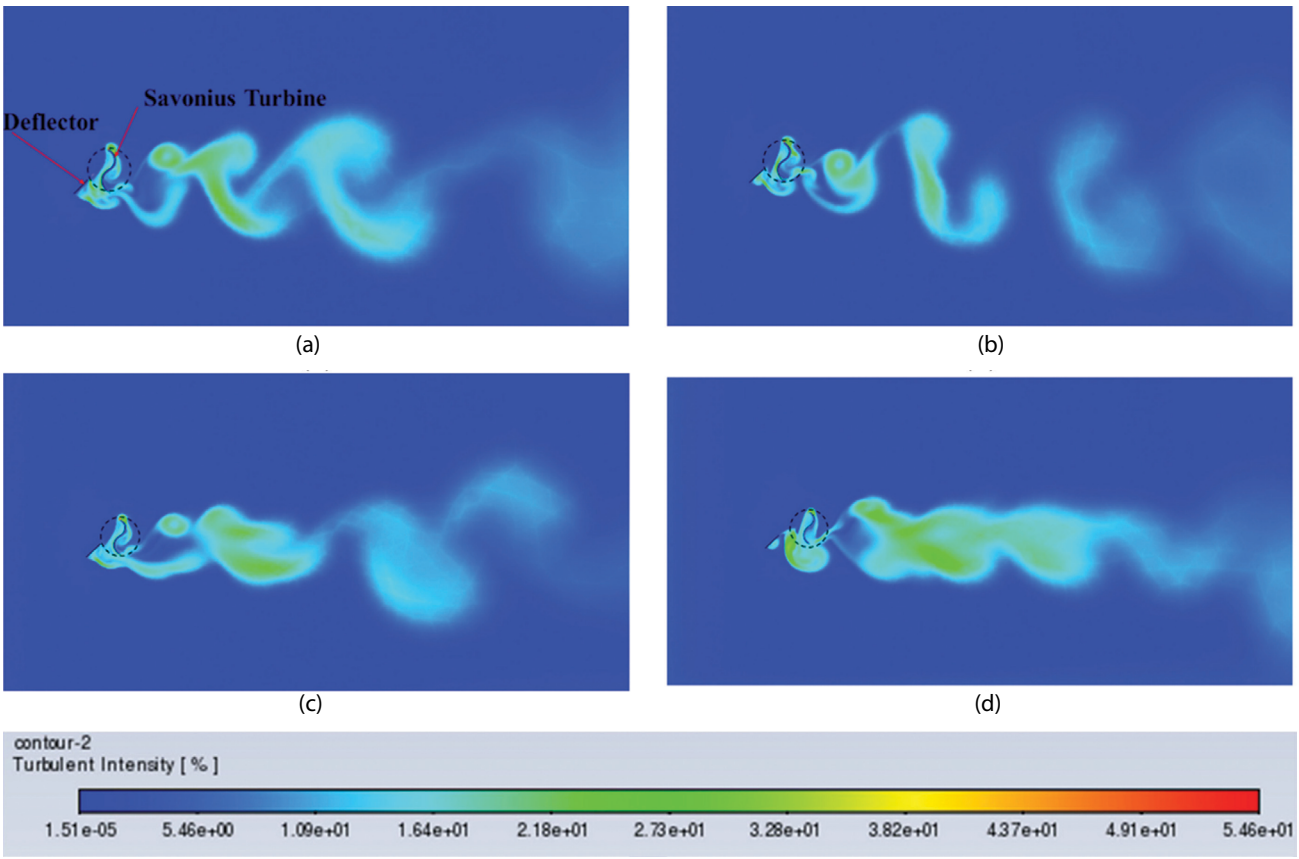

Figure 13 The turbulence intensity contour with a deflector (a) 0.22 m, (b) 0.23 m, (c) 0.24 m, (d) 0.33 m on TSR 0.800
Slika 13. Prikaz intenziteta turbulencije s deflektorom na udaljenosti (a) 0,22 m, (b) 0,23 m, (c) 0,24 m, (d) 0,33 m pri TSR-u od 0,800

length significantly influenced vortex formation and turbulence distribution, where shorter deflectors 0.22 and 0.23 m promoted more stable and energetic vortices. In comparison, longer deflectors 0.24 and 0.33 m produced larger but less coherent structures that dissipated more rapidly in the wake region.

The difference between the deflector distance yielding the maximum torque coefficient (Ct) and that producing the maximum power coefficient (Cp) reflects the inherent trade-off between torque generation and rotational speed in cross-flow Savonius turbines. At a deflector distance of 0.22 m, the deflector more effectively redirected the incoming flow toward the advancing blade while shielding the returning blade, resulting in a larger pressure differential and enhanced torque production, particularly at lower TSR. In contrast, the maximum Cp observed at a deflector distance of 0.23 m indicated a more balanced interaction between torque and angular velocity. At this configuration, the flow redirection remained sufficient to augment torque without inducing excessive drag or flow disturbance, allowing the rotor to operate at a slightly higher optimal TSR. Consequently, although the torque was marginally lower than at 0.22 m, the increased rotational speed led to higher power output. This behaviour highlighted configurations optimized for maximum Ct supported self-starting capability and low-TSR operation, while those optimized for maximum Cp were better suited for stable energy extraction under steady operating conditions.

4. CONCLUSION / *Zaključak*

This study conducts an evaluation of cross-flow Savonius turbine performance by incorporating deflector placement variations. The investigation considers multiple configurations, with deflectors positioned at distances of 0.22, 0.23, 0.24, and 0.33 m from the turbine. The numerical analysis of deflector use can improve turbine performance. In turbines with a 0.23 m deflector spacing, the largest increase in Ct and Cp values occur at a TSR of 0.696, with a 44% increase. The 0.22 m deflector placement and TSR 0.696 provide the most effective improvement in turbine performance, as evidenced by consistently higher Cp values. The 0.33 m configuration yields the lowest performance due to reduced hydrodynamic efficiency. Overall, the role of the deflector is most significant at low TSR conditions where Savonius turbines generally operate, while its impact diminishes at higher TSR > 0.900. The best performance for Ct was achieved at a deflector spacing of 0.22 m, with a TSR of 0.696, resulting in a final Ct value of 0.410. Meanwhile, the Cp value was achieved at a deflector spacing of 0.23 m at a TSR of 0.739, with a final Cp value of 0.289. These results show that proper deflector positioning can effectively increase the performance of a cross-flow Savonius turbine.

Author Contributions: Conceptualization, Methodology, Formal Analysis, Writing Original Draft, Writing Review and Editing, Funding Acquisition – D.S.; Investigation, Data Curation, Visualization, Writing Original Draft – R.A.A., M.A.M.; Formal Analysis, Review and Editing – M.M., T.T., M.L.H., N.A.R.; Writing Review and Editing – M.M., A.I., S.M.
Funding: This research funded by Institut Teknologi Sepuluh Nopember was under a Scientific Research scheme with contract number 1766/PKS/ITS/2025.
Conflict of interest: None.
Acknowledgments: The authors would like to convey their appreciation to Institut Teknologi Sepuluh Nopember.
Acknowledgement of AI or AI-assisted tools use: I have not used any AI or AI-assisted technologies to prepare this work.

REFERENCES / *Literatura*

[1] Satrio, D., Suntoyo, S., Erwandi, E., Albatinusa, F., Tuswan, T., & Hakim, M. L. (2023). The Benefit Using a Circular Flow Disturbance on the Darrieus Turbine Performance. *International Journal on Engineering Applications*, *11* (1), 55-63. https://doi.org/10.15866/irea.v11i1.22434

[2] Erwandi, E., Kasharjanto, A., Satrio, D., Rahuna, D., Suyanto, E. M., Mintarso, C. S. J., Irawanto, Z., & Ramadhani, M. A. (2024). Numerical Analysis of Resistance and Motions on Trimaran Floating Platform for Tidal Current Power Plant. *International Review on Modelling and Simulations*, *17* (1), 6-16. https://doi.org/10.15866/iremos.v17i1.24366

[3] Chen, H., Chang, L., Jin, Y., Wang, C., Xu, H., Cai, Z., & Liu, H. (2024). Design and performance study of oscillating hydrofoil-wave energy conversion device. *Journal of Marine Science and Technology*, *29* (4), 843-858. https://doi.org/10.1007/s00773-024-01023-1

[4] Rehman, S., Alhems, L. M., Alam, M. M., Wang, L., & Toor, Z. (2023). A review of energy extraction from wind and ocean: Technologies, merits, efficiencies, and cost. *Ocean Engineering*, 267, 113192. https://doi.org/10.1016/j.oceaneng.2022.113192

[5] Public Relations Office, Center for Marine Geological Survey and Mapping, Ministry of Energy and Mineral Resources (2025). *Potential of Indonesia's Ocean Energy*. Retrieved from https://geologi.esdm.go.id/media-center/potensi-energi-laut-indonesia

[6] Prabowo, Z. N., Mutianingsih, P., & Kurniawan, H. (2025). The Ocean Energy Potential in the Area of Early-Retirement Asset Coal-Fired Power Plants Owned by PT PLN (Persero). *IOP Conference Series: Earth and Environmental Science*, *1472* (1), 012030. https://doi.org/10.1088/1755-1315/1472/1/012030

[7] Mubarok, M. A., Arini, N. R., & Satrio, D. (2023). Optimization of Horizontal Axis Tidal Turbines Farming Configuration Using Particle Swarm Optimization (PSO) Algorithm. *Proceedings of the 2023 International Electronics Symposium (IES) IEEE* (pp. 19-25). https://doi.org/10.1109/IES59143.2023.10242450

[8] Satrio, D., Firdaus Yusri, M., Mukhtasor, Rahmawati, S., Junianto, S., & Musabikha, S. (2022). Numerical simulation of cross-flow Savonius turbine for locations with low current velocity in Indonesia. *Journal of the Brazilian Society of Mechanical Sciences and Engineering*, *44* (315), 1-11. https://doi.org/10.1007/s40430-022-03620-w

[9] Sun, Z. C., Li, D., Mao, Y. F., Feng, L., Zhang, Y., & Liu, C. (2022). Anti-cavitation optimal design and experimental research on tidal turbines based on improved inverse BEM. *Energy*, 239, 122263. https://doi.org/10.1016/j.energy.2021.122263

[10] Shouman, M. R., & Helal, M. M. (2023). Numerical investigation of improvement of counter rotating Savonius turbines performance with curtaining and fin addition on blade. *Alexandria Engineering Journal*, *75*, 233-242. https://doi.org/10.1016/j.aej.2023.05.002

[11] Satrio, D., Erwandi, & Rahuna, D. (2025). Investigation of enhanced peak lift performance and stall angle delay by attachment of Vortex Generators on blade surfaces of Vertical Axis Ocean Current Turbine. *Ocean Engineering*, 326, 120762. https://doi.org/10.1016/j.oceaneng.2025.120762

[12] Madi, M., Mukhtasor, Satrio, D., Tuswan, Ismail, A., Rafi, R., Yunesti, P., Buana, S. W., & Jarwinda. (2024). Experimental Study on the Effect of Foil Guide Vane on the Performance of a Straight-Blade Vertical Axis Ocean Current Turbine. *Naše more*, 71. https://doi.org/10.17818/NM/2024/1.1

[13] Satrio, D., Putra, D. J., Dhanistha, W. L., Utama, I. K. A. P., Putranto, T., Hayati, N., Muharja, M., & Madi, M. (2024). A Numerical Study of the Effect of Depth Immersion and Rotation Direction on the Performance of Cross-Flow Savonius Turbines. *Pomorstvo*, *38* (2), 250-262. https://doi.org/10.31217/p.38.2.7

[14] Ramdhani, M. A., & Cho, I. H. (2024). Optimization of a Savonius hydrokinetic turbine for performance improvement: A comprehensive analysis of immersion depth and rotation direction. *Ocean Systems Engineering*, *14* (2), 41-56. https://doi.org/10.12989/ose.2024.14.2.041

[15] Payambarpour, S. A., Najafi, A. F., & Magagnato, F. (2020). Investigation of deflector geometry and turbine aspect ratio effect on 3D modified in-pipe hydro Savonius turbine: Parametric study. *Renewable Energy*, 148, 44-59. https://doi.org/10.1016/j.renene.2019.12.002

[16] Badrul Salleh, M., Kamaruddin, N. M., How Tion, P., & Mohamed-Kassim, Z. (2021). Comparison of the power performance of a conventional Savonius turbine with various deflector configurations in wind and water. *Energy Conversion and Management*, 247, 114726. https://doi.org/10.1016/j.enconman.2021.114726

[17] Golecha, K., Eldho, T. I., & Prabhu, S. V. (2011). Influence of the deflector plate on the performance of modified Savonius water turbine. *Applied Energy*, *88* (9), 3207-3217. https://doi.org/10.1016/j.apenergy.2011.03.025

[18] Talukdar, P. K., Sardar, A., Kulkarni, V., & Saha, U. K. (2018). Parametric analysis of model Savonius hydrokinetic turbines through experimental and computational investigations. *Energy Conversion and Management*, 158, 36-49. https://doi.org/10.1016/j.enconman.2017.12.011

[19] Setiawan, P. A., Yuwono, T., & Widodo, W. A. (2019). Effect of a circular cylinder in front of advancing blade on the savonius water turbine by using transient simulation. *International Journal of Mechanical and Mechatronics Engineering*, *19* (1), 151-159.

[20] Madi, M., Yanda, R., Untoro, M. C., Satrio, D., Tuswan, T., Gufran, M., & Bangsa, N. (2025). Experimental Investigation of Convergent Flow Disturbances for Performance Enhancement of Vertical- Axis Ocean Current Turbine at Low Current Speed in Indonesia. *Transactions on Maritime Science*, *14* (1), 1-20. https://doi.org/10.7225/toms.v14.n01.012

[21] Ogawa, T., & Yoshida, H. (1986). The effects of a deflecting plate and rotor end plates on performances of Savonius-type wind turbine. *Bulletin of JSME*, 29, 2115-2121. https://doi.org/10.1299/jsme1958.29.2115

[22] Salleh, M. B., Kamaruddin, N. M., Mohamed-kassim, Z., & Bakar, E. A. (2021). Experimental investigation on the characterization of self-starting capability of a 3-bladed Savonius hydrokinetic turbine using deflector plates. *Ocean Engineering*, 228, 108950. https://doi.org/10.1016/j.oceaneng.2021.108950

[23] Satrio, D., Adityaputra, K. A., Suntoyo, S., Silvianita, S., Dhanistha, W. L., Gunawan, T., Muharja, M., & Felayati, F. M. (2023). The influence of deflector on the performance of cross-flow Savonius turbine. *International Review on Modelling and Simulations*, *16* (1), 27-34. https://doi.org/10.15866/iremos.v16i1.22763

[24] Ismail, M. F., & Vijayaraghavan, K. (2015). The effects of aerofoil profile modification on a vertical axis wind turbine performance. *Energy*, 80, 20-31. https://doi.org/10.1016/j.energy.2014.11.034

[25] Marsh, P., Ranmuthugala, D., Penesis, I., & Thomas, G. (2017). The influence of turbulence model and two and three-dimensional domain selection on the simulated performance characteristics of vertical axis tidal turbines. *Renewable Energy*, 105, 106-116. https://doi.org/10.1016/j.renene.2016.11.063

[26] Satrio, D., Utama, I. K. A. P., & Mukhtasor. (2018). The influence of time step setting on the CFD simulation result of vertical axis tidal current turbine. *Journal of Mechanical Engineering and Sciences*, *12* (1), 3399-3409. https://doi.org/10.15282/jmes.12.1.2018.9.0303

[27] Yin, T., Pavesi, G., Pei, J., & Yuan, S. (2021). Numerical investigation of unsteady cavitation around a twisted hydrofoil. *International Journal of Multiphase Flow*, 135, 103506. https://doi.org/10.1016/j.ijmultiphaseflow.2020.103506